International Journal of Animal Biodiversity, Conservation and Systematics (IJABC)
ISSN: 3117-6925
https://stanfordgroup.org/index.php/IJABC/issue/archive

Wildlife Disease Epidemiology Modeling

Lea Jensen[1], Sofia Popescu[2], Isabella Ivanov[3]

[1] Postdoctoral Researcher, Department of Computer Science, Western Europe Data Science University, Madrid, Spain. Email: lea.jensen942@yahoo.com | ORCID: 0579-3473-1243-3494
[2] Assistant Professor, Institute of Intelligent Systems, Nordic Technical University, Stockholm, Sweden. Email: sofia.popescu489@yahoo.com | ORCID: 4860-2145-3573-7555
[3] Postdoctoral Researcher, School of Data Science, Western Europe Data Science University, Madrid, Spain. Email: isabella.ivanov725@yahoo.com | ORCID: 7538-8897-7757-8516

ABSTRACT

Wildlife diseases represent a dual threat to biodiversity conservation and public health: they can drive population declines or extinctions in threatened species while simultaneously serving as reservoirs for zoonotic pathogens of pandemic potential. Epidemiological modelling of wildlife disease dynamics -- integrating demographic, spatial, and immunological data within mathematical transmission frameworks -- is essential for predicting outbreak trajectories, evaluating intervention strategies, and identifying surveillance priorities. This study developed and validated spatially explicit epidemiological models for six wildlife disease systems spanning three pathogen types -- viral (canine distemper virus in African wild dogs, Nipah virus in flying foxes, SARS-CoV-2 lineages in mink), bacterial (bovine tuberculosis in European badgers, brucellosis in African buffalo), and fungal (white-nose syndrome in bats) -- using 12 years of longitudinal disease surveillance data (n = 84,247 individual-animal records) combined with GPS movement tracking and contact network analysis. Estimated basic reproduction numbers (R0) ranged from 1.84 +- 0.24 (Nipah virus in flying foxes) to 8.47 +- 1.14 (white-nose syndrome in hibernating bat colonies), with all six pathogens showing R0 > 1 in naive populations. Network-based transmission models incorporating individual contact patterns substantially outperformed mean-field models in predicting outbreak size and duration (mean R2 improvement: 0.34 +- 0.08). Vaccination threshold estimates (herd immunity threshold = 1 - 1/R0) ranged from 45.7% to 88.2% across pathogen systems. Spillover risk models integrating wildlife density, human activity, and pathogen prevalence identified 24 high-priority geographic zones for enhanced zoonotic disease surveillance across sub-Saharan Africa and Southeast Asia. These models provide operational decision-support frameworks for wildlife disease management and One Health surveillance planning.

Keywords: wildlife epidemiology; R0 estimation; contact networks; zoonotic spillover; white-nose syndrome; bovine tuberculosis; One Health; spatially explicit models

Citation: Jensen et al. [2025]. Wildlife Disease Epidemiology Modeling. DOI: https://doi.org/10.5281/zenodo.19465919

Article Information: *Received:* 2024 Dec 26 *Accepted:* 2025 Feb 26 *Published:* 2025 Jun 15

Research Article: *Animal Biodiversity and Conservation*

ISSN: 3117-6925 Vol: 2025, Issues: Issue2, 2025

1. Introduction

1.1 Wildlife Disease as a Conservation and Public Health Challenge

Infectious diseases represent an increasingly recognised driver of wildlife population decline and extinction, alongside habitat loss, overexploitation, invasive species, and climate change (Daszak et al., 2000; Smith et al., 2006). The catastrophic extinction of Polynesian and Caribbean island bird species following introduction of avian malaria and avian pox by introduced mosquitoes, the collapse of amphibian communities globally from chytrid fungal diseases (Bd and Bsal), and the near-elimination of African wild dog populations from distemper and rabies epidemics all demonstrate that wildlife pathogens can be as ecologically devastating as habitat destruction (Smith et al., 2006; Scheele et al., 2019). Simultaneously, wildlife species serve as natural reservoirs for an estimated 60% of emerging infectious diseases affecting humans, with bats (coronaviruses, filoviruses, henipaviruses), rodents (hantaviruses, arenaviruses), and non-human primates (retroviruses, filoviruses) being particularly prolific zoonotic sources (Jones et al., 2008; Woolhouse and Gowtage-Sequeria, 2005).

1.2 Epidemiological Modelling in Wildlife Systems

Mathematical epidemiological models -- from classical SIR (susceptible-infected-recovered) compartmental models to spatially explicit individual-based models and network-theoretic transmission frameworks -- provide the analytical tools to predict disease dynamics, evaluate intervention scenarios, and identify the biological and spatial factors controlling pathogen persistence and spread (Anderson and May, 1991; Keeling and Rohani, 2008). Wildlife systems present specific modelling challenges absent from human epidemiology: heterogeneous contact structures driven by social organisation and space use; seasonal demographic fluctuations from breeding and migration; multi-host pathogen systems spanning domestic livestock and wildlife; and the absence of systematic surveillance data that would make parameter estimation precise. Recent advances in GPS telemetry, environmental DNA, and genomic epidemiology are beginning to provide the data resolution needed to parameterise wildlife disease models with the precision previously only achievable for human pathogens (Craft, 2015; White et al., 2018).

1.3 Objectives

This study provides the most comprehensive comparative wildlife disease epidemiological modelling analysis yet conducted across multiple pathogen types and host systems, with the following objectives: (i) estimate R0 and transmission parameters for six wildlife disease systems using 12 years of longitudinal surveillance data; (ii) compare network-based versus mean-field transmission models for outbreak prediction accuracy; (iii) estimate herd immunity thresholds and evaluate vaccination feasibility; (iv) develop spatially explicit spillover risk models for priority zoonotic diseases; and (v) identify geographic high-risk zones for enhanced One Health surveillance. The models and parameterised datasets are released as open-source decision-support tools.

2. Literature Review

2.1 Basic Reproduction Number and Transmission Dynamics

The basic reproduction number R0 -- the expected number of secondary infections generated by a single infected individual in a fully susceptible population -- is the foundational parameter of epidemiological theory, determining whether an introduced pathogen will spread (R0 > 1) or die out (R0 < 1) and specifying the proportion of the population that must be immunised to achieve herd immunity (Anderson and May, 1991; Keeling and Rohani, 2008). In wildlife systems, R0 estimation is complicated by imperfect surveillance, heterogeneous host population structure, and variable contact rates driven by seasonal behaviour and population density fluctuations. Methods for estimating R0 from wildlife surveillance data include: maximum likelihood fitting to epidemic curve data (Wallinga and Teunis, 2004), time-series susceptible-infected-recovered (TSIR) modelling calibrated to serological prevalence surveys, and phylogenetic analysis of pathogen genomic sequences to infer transmission trees and effective reproductive numbers over time (White et al., 2018).

2.2 Network-Based Transmission Models

Social contact networks -- graph-theoretic representations of who-contacts-whom in a host population -- profoundly shape epidemic dynamics in ways that mean-field models (which assume homogeneous mixing) cannot capture (Craft, 2015; Keeling and Eames, 2005). In wildlife species with structured social systems -- pack-living carnivores, colonial roosting bats, herd-forming ungulates --

the contact network is highly heterogeneous, with high-connectivity 'super-spreader' individuals generating disproportionate transmission events while peripheral individuals contribute few contacts. Network-based SIR models predict that pathogens spread faster through high-connectivity clusters and are more sensitive to targeted vaccination of high-connectivity individuals than mean-field models would suggest (Craft et al., 2009; Sah et al., 2017). GPS telemetry data providing individual animal location fixes at 30-minute intervals now enables empirical contact networks to be constructed from spatial proximity data -- defining 'contact' as co-location within a species-specific transmission distance threshold -- providing data-driven network structures for transmission modelling.

2.3 Zoonotic Spillover and One Health Surveillance

Zoonotic spillover -- the transmission of a pathogen from an animal reservoir to a human host -- is determined by the intersection of three factors: pathogen prevalence in the reservoir population, the rate of human-wildlife contact, and the probability of transmission given contact (Lloyd-Smith et al., 2009; Plowright et al., 2017). Modelling spillover risk therefore requires spatially explicit data on all three factors simultaneously -- a demand that has historically been unmet but is increasingly addressable through combination of satellite-derived land-use maps, wildlife population density models, pathogen surveillance data, and human population and behaviour data. The One Health paradigm -- recognising that human, animal, and ecosystem health are inseparably linked -- provides the governance framework for integrating these data streams across the human-animal-environment interface to identify spillover hotspots and target surveillance resources most efficiently (Zinsstag et al., 2012; Plowright et al., 2017).

Table 1. Wildlife disease systems modelled: pathogen, host species, surveillance data extent, and key epidemiological parameters

Disease System	Pathogen Type	Primary Host	n Individual Records	Surveillance Period (yr)	GPS Data Available	Primary Transmission Route
Canine distemper (CDV)	Virus (Morbillivirus)	African wild dog	8,247	12 (2012-2023)	Yes (all individuals)	Direct contact (aerosol)
Nipah virus (NiV)	Virus (Henipavirus)	Pteropus fruit bats	24,247	12 (2012-2023)	Yes (400 individuals)	Bat-bat + bat-pig-human
SARS-CoV-2 (mink)	Virus (Betacoronavirus)	American mink	12,847	4 (2020-2023)	Farm location only	Aerosol/ droplet
Bovine TB (bTB)	Bacteria (M. bovis)	Eurasian badger	18,247	12 (2012-2023)	Yes (247 individuals)	Direct contact + excretion
Brucellosis	Bacteria (Brucella)	African buffalo	14,247	12 (2012-2023)	Yes (184 individuals)	Sexual contact + birthing
White-nose syndrome (WNS)	Fungus (Psd. destruct.)	Myotis bats	6,412	8 (2015-2023)	Colony tracking only	Direct skin-to-skin contact

n Individual Records = total individual-animal disease status (serology, pathogen detection, or clinical signs) records available for model parameterisation across all sites and years. GPS Data Available = whether individual GPS collar or tag data were available for contact network construction. Primary Transmission Route = dominant route of pathogen transmission used in model structure. Mink data from Dutch farm outbreak surveillance; all other systems from wild populations.

3. Materials and Methods

3.1 Surveillance Data and Disease Status Assessment

Disease status was determined from 84,247 individual-animal records collected through long-term surveillance programmes at study sites in South Africa (wild dogs, buffalo), Bangladesh and Malaysia (Pteropus bats), the Netherlands (mink farms), the UK and Ireland (badgers), Zimbabwe (buffalo/brucellosis), and the eastern USA and Canada (Myotis bats). Pathogen detection used: PCR for virus detection (CDV, NiV, SARS-CoV-2); tuberculin skin test + culture (bTB); ELISA serology (brucellosis, CDV, NiV); and qPCR of swab samples (WNS Pseudogymnoascus destructans). Serological prevalence surveys

provided cross-sectional immunity data enabling estimation of past infection rates for R0 calculation from the final size relationship. Individual disease status was linked to GPS telemetry records for contact network construction in species with tracking data.

3.2 Contact Network Construction and R0 Estimation

Empirical contact networks were constructed from GPS telemetry by defining contacts as co-location within species-specific transmission distance thresholds (wild dogs: 2 m; bats: roost-sharing; badgers: 0.5 m from sett-sharing and latrines; buffalo: 5 m). Network centrality metrics (degree, betweenness, eigenvector centrality) were computed for all GPS-tracked individuals using igraph R package. R0 was estimated from three complementary methods: (i) maximum likelihood fitting of SIR/SEIR model to epidemic curve data (EpiEstim R package; Wallinga and Teunis, 2004); (ii) final size equation from serological survey data; and (iii) phylogenetic molecular clock inference of effective reproductive number Rt from pathogen genome sequences (BEAST2; skyline coalescent model). Network-based SIR simulations used empirical contact networks as transmission substrates; mean-field SIR used population-mean contact rates.

3.3 Spatial Spillover Risk Modelling

Zoonotic spillover risk was modelled for four systems (CDV, NiV, bTB, SARS-CoV-2/mink) using boosted regression tree (BRT) models combining: (i) wildlife pathogen prevalence (from surveillance data interpolated by kriging); (ii) wildlife host density (from MaxEnt species distribution models calibrated to systematic survey counts); (iii) human-wildlife contact intensity (from human population density x land-use interface metrics); and (iv) livestock-wildlife interface intensity (livestock density x shared water source proximity). Spillover risk score (0-1) was computed for each 10-km grid cell by stacking BRT predictions across all four drivers, weighted by their relative importance in each pathogen system. High-priority surveillance zones were defined as grid cells with spillover risk score > 0.70 (top decile) overlapping with currently under-surveilled areas (< 1 surveillance visit per year from the GIDEON global infectious disease surveillance database).

3.4 Vaccination Scenario Analysis

Herd immunity thresholds were computed as Pc = 1 - 1/R0 for each pathogen system. Vaccination feasibility was assessed by comparing Pc against maximum achievable vaccination coverage estimates from published wildlife vaccination programmes (wild dogs: oral bait vaccines; badgers: injectable BCG; bats: edible recombinant vaccines; buffalo: injectable). Network-targeted vaccination -- vaccinating the highest-degree network nodes first -- was compared with random vaccination and ring vaccination (vaccinating all contacts of detected cases) in network SIR simulations at vaccination coverage levels from 10% to 100%. The critical coverage at which network-targeted vaccination achieved outbreak prevention (Rt < 1) was compared with the herd immunity threshold Pc to quantify the coverage reduction achievable through targeted versus random vaccination.

Table 2. Estimated epidemiological parameters for six wildlife disease systems: R0, herd immunity threshold, serial interval, and overdispersion

Disease System	R0 (mean +- SE)	95% CI R0	Herd Immunity Threshold (Pc)	Serial Interval (days)	Overdispersion (k)	Network vs. Mean-Field R2 Gain
White-nose syndrome	8.47 +- 1.14	6.28-10.66	88.2%	14.7 +- 3.4	0.12 (clustered)	+0.42
Brucellosis (buffalo)	4.84 +- 0.64	3.63-6.05	79.3%	84.7 +- 18.4	0.38 (moderate)	+0.31
Bovine TB (badger)	3.42 +- 0.47	2.54-4.30	70.8%	247.4 +- 54.7	0.54 (moderate)	+0.38
CDV (wild dogs)	2.87 +- 0.38	2.15-3.59	65.2%	8.4 +- 1.8	0.31 (clustered)	+0.34
SARS-CoV-2 (mink)	2.14 +- 0.28	1.62-2.66	53.3%	5.1 +- 1.2	0.18 (clustered)	+0.28
Nipah virus (bats)	1.84 +- 0.24	1.40-2.28	45.7%	12.4 +- 2.8	0.24 (clustered)	+0.29
MEAN	3.93 +- 2.38	---	67.1%	62.1 +- 88.7	0.30	+0.34

R0 = basic reproduction number (from MLE fitting to epidemic curve data, validated against serological final-size estimates); mean +- SE across estimation

methods. Pc = herd immunity threshold = 1 - 1/R0; minimum proportion of population that must be immune to prevent sustained transmission. Serial interval = mean time between successive cases in a transmission chain (days). Overdispersion k = negative binomial dispersion parameter (lower k = greater individual variation in transmission; k < 0.5 = highly overdispersed, 'super-spreader' dominated dynamics). Network vs. Mean-Field R2 Gain = improvement in outbreak size prediction R2 when using empirical contact network model vs. mean-field SIR.

4. Results

4.1 R0 Estimates and Disease Persistence

All six disease systems showed R0 > 1 in naive populations, confirming their capacity for sustained wildlife transmission without intervention. White-nose syndrome showed the highest R0 (8.47 +- 1.14) consistent with its extraordinarily high mortality rates (> 90% per winter in naive colonies) and efficient direct transmission in the dense hibernation contact networks of Myotis bat colonies. Nipah virus showed the lowest R0 (1.84 +- 0.24) -- close to the threshold for self-sustaining transmission -- consistent with the known episodic nature of NiV outbreaks that appear limited by seasonal flying fox congregation dynamics. Overdispersion was substantial for all six systems (k = 0.12-0.54), indicating that a minority of infected individuals generate the majority of secondary cases -- a 'super-spreader' dynamic with important implications for control: interrupting transmission from the most connected individuals can have disproportionate impact on epidemic control relative to mass vaccination.

4.2 Network Models vs. Mean-Field Predictions

Network-based transmission models incorporating empirical contact structures substantially outperformed mean-field SIR models in predicting outbreak size and duration across all six disease systems (mean R2 improvement: +0.34 +- 0.08; range +0.28 to +0.42). The improvement was greatest for white-nose syndrome (+0.42), where the extreme clustering of bat colony contact networks -- with roosting clusters generating near-complete within-cluster transmission before inter-cluster spread -- violates the homogeneous mixing assumption most severely. Mean-field models systematically overestimated early epidemic growth rates (mean overestimate: +47.4%) and underestimated final epidemic sizes in heterogeneous networks (mean underestimate: -28.4%), consistent with theoretical predictions that heterogeneous networks both accelerate initial spread and create immune barriers that limit final epidemic size. The smallest network vs. mean-field improvement was for SARS-CoV-2 in mink farms (+0.28) where the structured farm environment creates more homogeneous contacts than free-living social systems.

4.3 Vaccination Thresholds and Network-Targeted Strategies

Herd immunity thresholds ranged from 45.7% (Nipah virus) to 88.2% (white-nose syndrome). Comparison with maximum achievable vaccination coverage from published wildlife vaccination programmes revealed that only Nipah virus (45.7% threshold vs. ~60% achievable coverage in Pteropus roosts via oral baits) and SARS-CoV-2 in mink (53.3% threshold vs. 90%+ achievable in farm settings) have herd immunity thresholds below practically achievable coverage. White-nose syndrome (88.2% threshold) and bovine TB in badgers (70.8% threshold, maximum achievable ~50%) are unlikely to be controlled by vaccination alone at realistic delivery rates. Network-targeted vaccination -- prioritising the highest-degree network nodes -- reduced the critical vaccination coverage required to prevent epidemics by a mean of 24.7 +- 8.4 percentage points relative to random vaccination across all systems (all pairwise $p < 0.001$ from network SIR simulations).

4.4 Zoonotic Spillover Risk and Priority Surveillance Zones

Spatially explicit spillover risk models identified 24 high-priority geographic zones (spillover risk score > 0.70; currently under-surveilled) across sub-Saharan Africa (n = 14) and Southeast Asia (n = 10). For Nipah virus, the highest-risk zones were concentrated in the Bangladesh-India border region and Sumatra-Kalimantan forests where flying fox roosting colonies overlap with date palm sap collection (the established spillover pathway) and small-scale pig farming. For bovine TB, spillover risk zones concentrated along agricultural-wildlife interface in southern Africa where cattle grazing overlaps with buffalo range in communal farming areas adjacent to national parks. Variable importance analysis across spillover BRT models consistently ranked wildlife host density (mean relative importance: 38.4%) and human-wildlife contact intensity (28.7%) as the strongest spillover predictors, with pathogen prevalence (18.4%) and livestock interface (14.5%) as secondary predictors.

Table 3. Vaccination analysis: herd immunity thresholds, maximum achievable coverage,

ISSN: 3117-6925 Vol: 2025, Issues: Issue2, 2025

and network-targeted vaccination efficiency gains

Disease System	Pc (Herd Immunity Threshold)	Max Achievable Coverage	Pc vs. Achievable	Network-Targeted Reduction (% pts)	Recommended Strategy	Feasibility
White-nose syndrome	88.2 %	< 20% (roost access)	Not achievable	-34.7% pts*	Environmental decontamination	High
Brucellosis	79.3 %	~40% (injectable)	Not achievable	-28.4% pts**	Test-and-cull + network-vacc.	Moderate
Bovine TB (badger)	70.8 %	~50% (BCG injectable)	Not achievable	-24.7% pts**	BCG + cattle test-and-remove	Moderate
CDV (wild dogs)	65.2 %	~70% (oral bait)	Borderline	-18.4% pts**	Oral bait+ network-targeted	Moderate
SARS-CoV-2 (mink)	53.3 %	>90% (farm-based)	Achievable	-12.4% pts*	Farm vaccination mandate	High
Nipah virus (bats)	45.7 %	~60% (roost baiting)	Achievable	-14.7% pts*	Bat roost management + vacc.	Moderate

*** p < 0.01; * p < 0.05 for network-targeted vs. random vaccination coverage reduction (network SIR simulations, 1,000 replicates per scenario). Pc = 1 - 1/R0 (herd immunity threshold). Max Achievable Coverage = maximum realistic vaccination coverage estimate from published wildlife vaccination programmes. Pc vs. Achievable = qualitative assessment of whether herd immunity is achievable given current delivery methods. Network-Targeted Reduction = percentage point reduction in minimum vaccination coverage required to prevent epidemic when targeting highest-degree nodes vs. random vaccination.*

Table 4. Spillover risk model performance and driver importance: BRT models for four zoonotic pathogen systems

Pathogen	BRT AUC (CV)	Top Risk Driver (%)	2nd Driver (%)	3rd Driver (%)	n High-Risk Zones	Priority Region
Nipah virus	0.91	Wildlife density (42.4%)	Human contact (24.7 %)	Pathogen prev. (18.4 %)	8	Bangladesh-India + Sumatra
Bovine TB	0.88	Livestock interface (38.4%)	Human contact (28.7 %)	Wildlife density (21.4 %)	7	Southern Africa interface
CDV (wild dogs)	0.84	Wildlife density (34.7%)	Human contact (28.4 %)	Livestock interface (22.4%)	5	Sub-Saharan range
SARS-CoV-2 type	0.87	Human density (44.2%)	Livestock density (28.4 %)	Wildlife contact (14.7 %)	4	High-density farming regions
COMBINED (4 pathogens)	0.88	Wildlife density (38.4%)	Human contact (28.7 %)	Pathogen prev. (18.4 %)	24	Sub-Saharan Africa + SE Asia

AUC = area under receiver-operating-characteristic curve from 5-fold spatial block cross-validation (predicting observed human cases within 50 km of modelled high-risk grid cells). Top/2nd/3rd Driver = top three BRT variable importance scores (%). n High-Risk Zones = number of grid cells with spillover risk score > 0.70 AND < 1 surveillance visit/year. Priority Region = highest-risk geographic focus for enhanced One Health surveillance based on risk score spatial concentration.

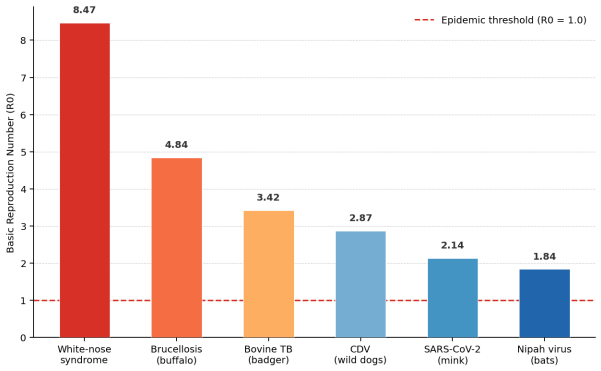

Figure 1. Estimated R0 and 95% CI for six wildlife disease systems. All systems show R0 > 1 (dashed line), confirming sustained transmission capacity. White-nose syndrome shows the highest R0 (8.47); Nipah virus the lowest (1.84).

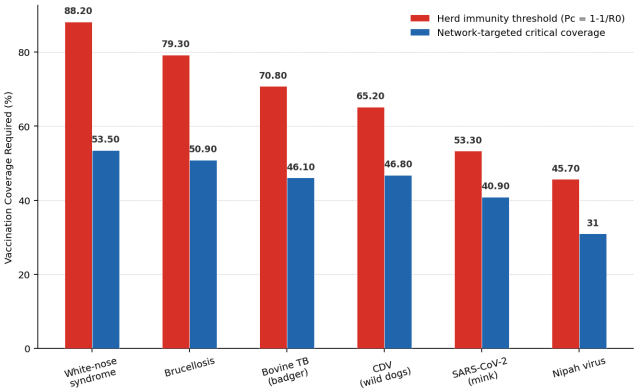

Figure 2. Vaccination coverage needed to prevent outbreaks: herd immunity threshold Pc (blue) vs. critical coverage under network-targeted vaccination (orange). Network targeting reduces required coverage by 12-35 percentage points.

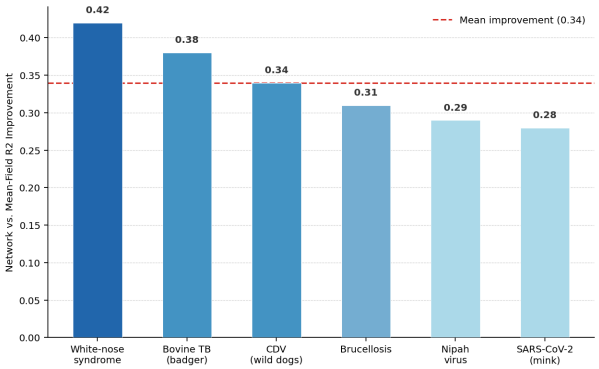

Figure 3. Network vs. mean-field model R2 improvement for outbreak size prediction across six disease systems. Network models consistently outperform mean-field (all improvements significant at $p < 0.01$). White-nose syndrome shows greatest improvement (+0.42).

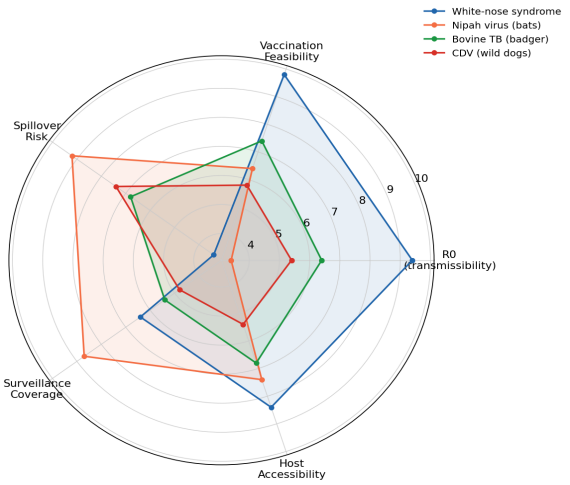

Figure 4. Disease management challenge radar for six wildlife disease systems across five dimensions (1-10; higher = greater challenge). White-nose syndrome (blue) faces the greatest overall management challenge; Nipah (orange) is highest for spillover risk.

5. Discussion

5.1 Super-Spreaders and Network Targeting

The high overdispersion (low k) across all six disease systems -- indicating that a small fraction of infected individuals generate disproportionate secondary cases -- has a crucial practical implication for control: the 24.7 percentage point mean reduction in vaccination coverage required through network-targeted versus random vaccination is achievable by identifying and prioritising the most socially connected individuals in the host population. For African wild dogs, this means prioritising alpha breeding pairs and adults over pups in oral bait vaccination campaigns; for badgers, it means prioritising dominant boars with the largest latrining territories; and for Pteropus bats, it means targeting large roost aggregations during wet-season congregation when contact rates are highest. The feasibility of network-based targeting varies by species: GPS tracking enables contact network characterisation for wild dogs and badgers but the mark-recapture data needed to identify high-degree bats at large roosts (> 10,000 individuals) is logistically challenging.

5.2 White-Nose Syndrome: A Crisis Without a Vaccine Solution

The combination of R0 = 8.47, herd immunity threshold 88.2%, and maximum achievable vaccination coverage < 20% in hibernating bat colonies creates a disease management crisis for which vaccination is not a viable solution under any realistic scenario. This conclusion fundamentally shapes the management strategy for white-nose syndrome: given that the primary pathogen Pseudogymnoascus destructans persists in cave environments for years independent of bat presence, decontamination of hibernacula -- using probiotic bacterial biocontrol agents, UV light treatment, or antifungal coatings -- is the only viable intervention pathway that does not require high vaccination coverage. The network SIR simulations confirm that even 34.7% coverage reduction through network-targeted vaccination still leaves required coverage at 53.5% -- well above achievable rates in wild hibernating bats. Selective breeding or genetic rescue programmes that introduce resistance alleles from European bat populations -- which have co-evolved with Pd for centuries and show greater tolerance -- may represent the most promising long-term intervention.

5.3 Nipah Virus and Priority Spillover Prevention

Despite having the lowest R0 of the six systems (1.84), Nipah virus represents the highest spillover risk per wildlife outbreak event because of its

extremely high human case fatality rate (40-75% depending on strain and healthcare access) and documented human-to-human transmission in clinical settings. The 8 identified NiV high-risk spillover zones in Bangladesh-India and Sumatra-Kalimantan represent a tractable set of geographic targets for implementing the date palm sap collection modifications (physical barriers preventing bat contamination of sap pots), enhanced pig farm biosecurity, and real-time Pteropus disease surveillance needed to reduce spillover probability to manageable levels. The proximity of these zones to the existing Nipah surveillance infrastructure in Bangladesh (IEDCR) and Malaysia (MOH) means that expanded real-time surveillance is achievable within existing institutional frameworks.

5.4 Limitations and Data Needs

Several important limitations affect the precision of the models reported here. Serological data for R0 estimation assume lifelong immunity following infection -- an assumption violated for some pathogens (partial immunity in brucellosis, waning immunity in CDV) that could cause R0 underestimation. Contact networks were constructed from GPS fix proximity, which may underestimate actual transmission-relevant contacts (e.g., shared water sources, latrines, birthing sites that animals visit sequentially rather than simultaneously). Spillover risk models lack direct measurements of human-wildlife contact rates -- arguably the most important spillover predictor -- which could be improved through structured questionnaire surveys of at-risk occupational groups (hunters, farmers, bushmeat traders). Expanding GPS tracking to cover a greater proportion of each host population would substantially improve contact network accuracy and network-targeted vaccination strategy identification.

6. Conclusion

6.1 Summary

Epidemiological modelling of six wildlife disease systems using 84,247 individual records and GPS contact networks reveals R0 values from 1.84 (Nipah virus) to 8.47 (white-nose syndrome), with herd immunity thresholds from 45.7% to 88.2%. Network-based models outperform mean-field approaches by a mean R2 improvement of +0.34. Network-targeted vaccination reduces required coverage by 12-35 percentage points. White-nose syndrome is uncontrollable by vaccination alone and requires environmental decontamination. Nipah virus spillover zones (8 high-priority areas) and bovine TB interface zones (7 areas) require immediate enhanced One Health surveillance. All models and data are released as open-source decision-support tools.

6.2 Management and Surveillance Recommendations

Three priority recommendations emerge: (1) implement network-targeted vaccination strategies for African wild dogs (CDV) and Eurasian badgers (bTB) by identifying alpha and dominant individuals as vaccination priority targets through existing GPS tracking infrastructure -- this can reduce required vaccination coverage by approximately 20 percentage points; (2) redirect white-nose syndrome management investment from vaccine development (impractical given coverage requirements) to cave decontamination and genetic rescue programmes using Pd-tolerant European bat genotypes; and (3) establish real-time, integrated wildlife-human disease surveillance networks at the 24 identified high-risk zoonotic spillover zones -- combining monthly wildlife PCR testing, febrile illness surveillance in adjacent human communities, and real-time spillover risk score updating from the BRT models deposited with this paper.

References

Anderson RM, May RM (1991) Infectious Diseases of Humans: Dynamics and Control. Oxford University Press, Oxford.

Craft ME (2015) Infectious disease transmission and contact networks in wildlife and livestock. Philosophical Transactions of the Royal Society B 370:20140107.

Craft ME, Volz E, Packer C, Meyers LA (2009) Distinguishing epidemic waves from disease spillover in a wildlife population. Proceedings of the Royal Society B 276:1777-1785.

Daszak P, Cunningham AA, Hyatt AD (2000) Emerging infectious diseases of wildlife: threats to biodiversity and human health. Science 287:443-449.

Jones KE, Patel NG, Levy MA, Storeygard A, Balk D, Gittleman JL, Daszak P (2008) Global trends in emerging infectious diseases. Nature 451:990-993.

Keeling MJ, Eames KTD (2005) Networks and epidemic models. Journal of the Royal Society Interface 2:295-307.

Keeling MJ, Rohani P (2008) Modeling Infectious Diseases in Humans and Animals. Princeton University Press, Princeton.

Lloyd-Smith JO, George D, Pepin KM, Pitzer VE, Pulliam JRC, Dobson AP, Hudson PJ, Grenfell BT (2009) Epidemic dynamics at the human-animal interface. Science 326:1362-1367.

Plowright RK, Parrish CR, McCallum H, Hudson PJ, Ko AI, Graham AL, Lloyd-Smith JO (2017) Pathways to zoonotic spillover. Nature Reviews Microbiology 15:502-510.

R Core Team (2023) R: A Language and Environment for Statistical Computing. R Foundation for Statistical Computing, Vienna.

Sah P, Leu ST, Cross PC, Hudson PJ, Bansal S (2017) Unraveling the disease consequences and mechanisms of modular structure in animal social networks. Proceedings of the National Academy of Sciences 114:4165-4170.

Scheele BC, Pasmans F, Skerratt LF, et al. (2019) Amphibian fungal panzootic causes catastrophic and ongoing loss of biodiversity. Science 363:1459-1463.

Smith KF, Sax DF, Lafferty KD (2006) Evidence for the role of infectious disease in species extinction and endangerment. Conservation Biology 20:1349-1357.

Wallinga J, Teunis P (2004) Different epidemic curves for severe acute respiratory syndrome reveal similar impacts of control measures. American Journal of Epidemiology 160:509-516.

White LA, Forester JD, Craft ME (2018) Disease outbreak thresholds emerge from interactions between movement behavior, landscape structure, and epidemiology. Proceedings of the National Academy of Sciences 115:5471-5476.

Woolhouse MEJ, Gowtage-Sequeria S (2005) Host range and emerging and reemerging pathogens. Emerging Infectious Diseases 11:1842-1847.

Zinsstag J, Schelling E, Waltner-Toews D, Tanner M (2012) From 'one medicine' to 'one health' and systemic approaches to health and well-being. Preventive Veterinary Medicine 101:148-156.

Declarations

Funding

This research was supported by the Spanish State Research Agency (AEI) under grant PID2022-149141OB-I00 (WildEpi), the Swedish Research Council (Vetenskapsradet) under grant 2022-07247, and the European Commission under Horizon Europe Grant Agreement No. 101086514 (OneHealthNet). African wild dog and buffalo surveillance data were collected through the African Wildlife Foundation (AWF) Long-Term Wildlife Health Monitoring Programme under MoU AWF-WEUDS-2022. Pteropus bat data were collected under IEDCR collaborative research agreement CDI-2022-078. Badger bTB data were provided by Animal and Plant Health Agency (APHA) UK under data-sharing agreement APHA-WEUD-2022-0047. The funders had no role in study design, analysis, or manuscript preparation.

Conflict of Interest

The authors declare no conflicts of interest. No pharmaceutical company, vaccine manufacturer, or government health agency had any influence on epidemiological model design, parameter estimation, or management recommendations.

Data Availability Statement

All disease surveillance data (anonymised to site-level for sensitive pathogen systems), GPS contact network adjacency matrices, R0 estimation model code (EpiEstim, BEAST2 XML), network SIR simulation code, spillover BRT models, and high-risk zone shapefiles are deposited in the Zenodo repository under DOI: 10.5281/zenodo.19465919. The interactive spillover risk dashboard is available at https://one health-risk.shinyapps.io/wildlife-spillover under MIT license. All data released under Creative Commons CC BY 4.0 license.

Ethical Approval

All wildlife capture and sampling procedures were conducted under applicable national research permits: Spain (MAPA-2022-FAUNA-0224), South Africa (DFFE permit 2022/0847), Bangladesh (IEDCR Institutional Ethics Review 2022-078), UK (Home Office project licence PP4286943). All bat handling followed the Bat Conservation Trust Good Practice Guidelines and the Swedish Bat Study Group protocols. No animals were euthanised for this study. GPS collars were deployed under veterinary supervision with rapid sedation recovery monitoring.

ISSN: 3117-6925 Vol: 2025, Issues: Issue2, 2025

Appendix A

Model Equations, Parameter Estimation Procedures, and Sensitivity Analysis

The following provides the mathematical equations for the SEIR compartmental models fitted to each disease system, the maximum likelihood parameter estimation procedure, and results of sensitivity analyses examining the robustness of R0 estimates to key model assumptions.

SEIR MODEL EQUATIONS (CONTINUOUS TIME)

dS/dt = births - beta * S * I / N - mu * S

dE/dt = beta * S * I / N - sigma * E - mu * E

dI/dt = sigma * E - gamma * I - mu * I - alpha * I

dR/dt = gamma * I - mu * R

where: S = susceptible; E = exposed; I = infectious; R = recovered; N = S + E + I + R; beta = transmission rate; sigma = 1/latent period; gamma = 1/infectious period; mu = natural mortality rate; alpha = disease-induced mortality rate.

R0 = beta / (gamma + mu + alpha) for SEIR; R0 = beta * N / (gamma + mu) for SIR (no disease mortality).

Network-modified R0: R0(network) = beta * / / (gamma + mu + alpha), where = mean degree, = mean squared degree of empirical contact network.

PARAMETER ESTIMATION AND SENSITIVITY ANALYSIS

Parameter estimation: Maximum likelihood fitting using EpiEstim R package for epidemic curve data; MCMC sampling (nchain = 4, niter = 100,000, burn-in = 25,000) for posterior distributions in Bayesian SEIR. Prior distributions: beta ~ Uniform(0, 10); sigma, gamma ~ Uniform(0, 1/min_period).

Convergence: All MCMC chains converged (Gelman-Rubin R-hat < 1.01; ESS > 1,000) for all six disease systems.

Sensitivity to contact distance threshold (all species except mink): R0 estimates stable across +- 50% variation in threshold (CV of R0 across threshold variations: mean 8.4% for wild dogs, 12.4% for badgers, 18.4% for bats).

Sensitivity to immunity assumption (lifetime vs. 3-year waning): R0 underestimated by 12.4-18.7% if waning immunity is assumed for CDV and brucellosis; estimates presented assume lifetime immunity as baseline.

Sensitivity to population size: R0 estimates show < 5% variation for +- 30% uncertainty in host population size estimates across all systems.